UNITED STATES DEPARTMENT OF THE INTERIOR

GEOLOGICAL SURVEY

GEOLOGY OF THE WHITEHORSE CALDERA AND CALDERA-FILL DEPOSITS, MALHEUR COUNTY, OREGON

By

James J. Rytuba, Scott A. Minor, and Edwin H. McKee

U.S. Geological Survey
Open-File Report 81-1092
1981

This report is preliminary and
has not been reviewed for conformity
with U.S. Geological Survey editorial
standards and stratigraphic nomenclature.

Table of Contents

	Page
Abstract	1
Introduction	1
Geology	1
Lithology of caldera-fill deposits and underlying volcanic rocks	6
Interpretation of caldera-fill volcanic rocks	8
Alteration mineralogy of caldera-fill deposits	10
Scanning Electron Microscopy observations	11
Uranium potential of caldera-fill deposits	18
Acknowledgments	18
References	19

Illustrations

		Page
Figure 1.	Location and age of calderas within southeast Oregon and north-central Nevada	2
2.	Generalized lithologic description of drill core	7
3.	SEM photo of erionite replacing a glass shard	12
4.	SEM photo of erionite and montmorillonite filling cavities in the rock	13
5.	SEM photo of phillipsite crystals	14
6.	SEM photo of clinoptilolite crystals filling cavities	15
7.	SEM photo of montmorillonite clay	16
8.	SEM photo of adularia and typical clay mineral morphology	17

Tables

Table 1.	Potassium-argon ages and analytical data for rhyolite dome samples of Willow Butte, tuff of Whitehorse Creek, and McDermitt tuff #5	3
2.	Partial chemistry of tuff of Whitehorse Creek, and Willow Butte and Whitehorse Butte ring domes	5

Plates
[in pockets]

Plate 1. Geology of the Whitehorse caldera
2. Geology and mineralogy of Whitehorse caldera sediments

GEOLOGY OF THE WHITEHORSE CALDERA AND CALDERA-FILL DEPOSITS, MALHEUR COUNTY, OREGON

By James J. Rytuba, Scott A. Minor, and Edwin H. McKee

ABSTRACT

The Whitehorse caldera is a Miocene collapse structure located in southwest Oregon, about 15 km northwest of the McDermitt caldera complex. Eruption of the peralkaline rhyolite tuff of Whitehorse Creek at 15.0±.3 m.y. resulted in the formation of a circular caldera 15 km in diameter. Rhyolite domes and associated flows were emplaced around the margin of the caldera and the caldera was subsequently filled with tuffaceous sediments and pyroclastic deposits.

Lithologic studies of a 135 m thickness of caldera-fill deposits encountered in a 226-m deep drill core document a quiet lacustrine sedimentation record repeatedly interrupted by rapid deposition of thick volcanic ash beds. The upper 37 m of the deposits consist primarily of diatomaceous earth with subordinate volcanic ash interbeds. A vertical zonation in alteration mineralogy occurs in the core with the upper 110 m being unaltered and the lower 35 m altered to zeolites and potassium feldspar. Phillipsite and erionite occur in the upper part of the alteration zone and with increasing depth clinoptilolite and potassium feldspar are present. Radiometric logging of the drill hole for uranium and thorium showed no anomalous zones.

INTRODUCTION

In southeast Oregon and north-central Nevada, several calderas and caldera complexes formed in the interval from 18.5 m.y. to 0.7 m.y. (Rytuba and Glanzman, 1979; Walker and Nolf, 1981). The oldest calderas occur within the McDermitt caldera complex and the youngest occurs at Newberry (MacLeod and others, 1981). The calderas become progressively younger to the northwest. This trend parallels the general northwest decrease in age of rhyolitic volcanism originally documented by Walker (1974). Deposits of mercury and uranium occur within the McDermitt caldera complex, whereas the other calderas have no recognized ore deposits associated with them. The Whitehorse caldera is a well-preserved Miocene collapse structure located about 15 km northwest of the McDermitt caldera complex (fig. 1). Alteration occurs locally along the margin of the Whitehorse caldera and recent core drilling by the U.S. Department of Energy has tested for uranium mineralization within the caldera. This paper focuses on the general geology of the Whitehorse caldera and presents the results of studies on the Whitehorse caldera-fill deposits sampled by the U.S. Department of Energy drill hole.

GEOLOGY

Eruption of the ash-flow tuff of Whitehorse Creek at 15.0±.3 m.y. (table 1) resulted in the formation of a circular collapse structure about 15 km in diameter (pl. 1). The tuff of Whitehorse Creek is about 1 m.y. younger than the youngest caldera forming ash-flow tuffs associated with the McDermitt caldera complex (tuffs 4 and 5, pl. 1). These older ash-flow tuffs

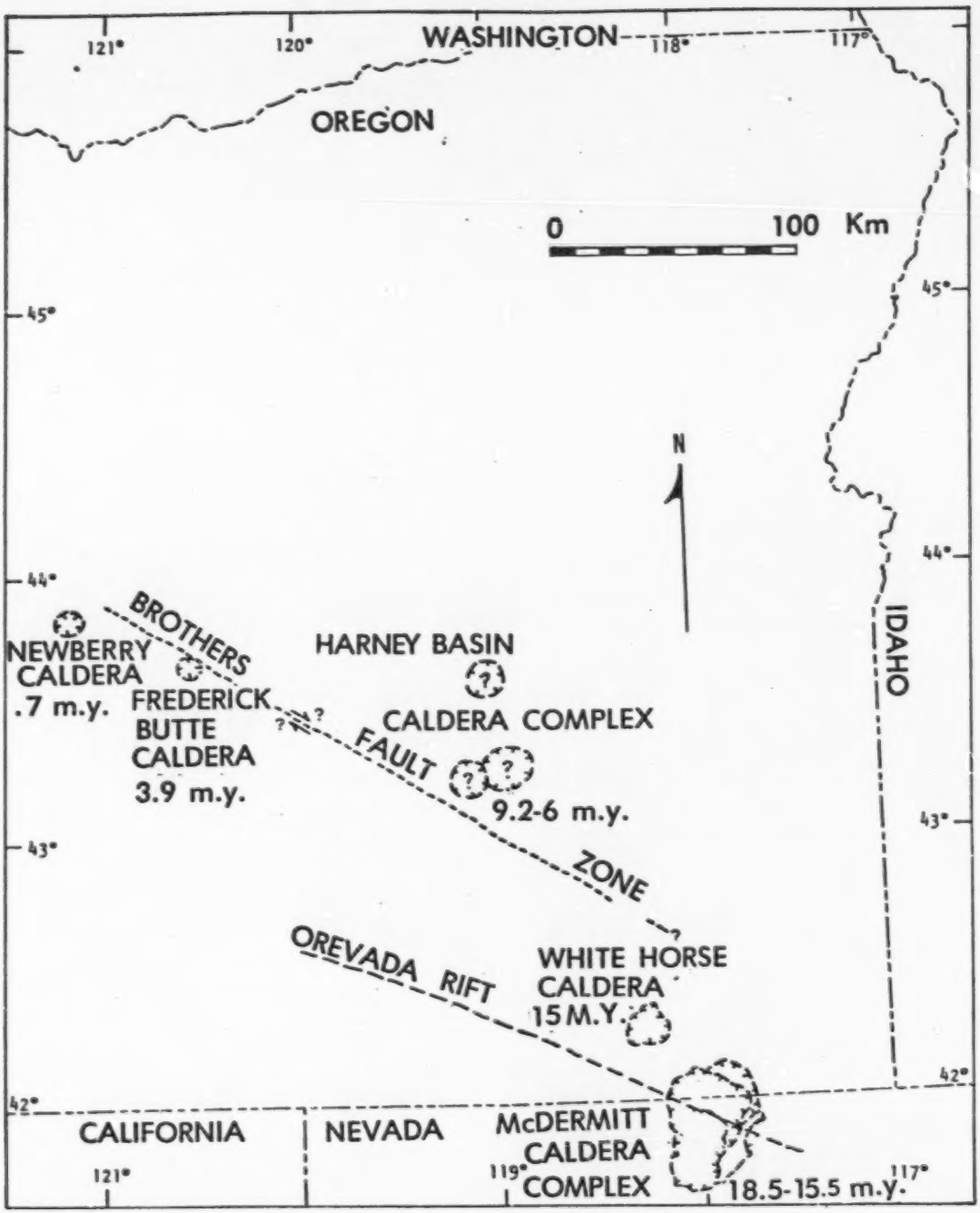

Figure 1.--Location and age of calderas within southeast Oregon and north-central Nevada. Distribution and age of Harney Basin and Frederick Butte calderas from Walker and Nolf (1981) and Newberry caldera from MacLeod and others (1981).

Table 1.--Potassium-argon ages and anlytical data for rhyolite dome sample of Willow Butte, tuff of Whitehorse Creek and McDermitt tuff #5

[Sanidine separates from fresh whole rock samples were made by heavy liquid and electromagnetic separation techniques. Splits of the pure mineral separate were analyzed for K_2O by a lithium metaborate fusion method and flame photometry and for Ar using isotope dilution methods and a Neir-type 60° sector, 15.2-cm-radius mass spectrometer. The precision of the date, shown as the ± value is the estimated analytical uncertainty at one standard deviation]

Name and field number	Mineral	K_2O percent	$^{40}Ar^{rad}$ mole/g	$^{40}Ar^{rad}/\ ^{40}Ar$	Age±m.y.
Willow Butte					
BO-21	Sanidine	5.98	1.1938×10^{-10}	52.5	13.8±0.3
Whitehorse tuff					
JR80-27	Sanidine	5.61	1.21656×10^{-10}	65.5	15.0±0.3
McDermitt #5					
p042-2	Sanidine	6.12	1.4326×10^{-10}	60.0	15.8±0.5

$\lambda_\varepsilon + \lambda'_\varepsilon = 0.581 \times 10^{-10} yr^{-1}$

$\lambda\beta = 4.962 \times 10^{10} yr^{-1}$

$40K = 1.167 \times 10^{14}$ mole/mole

rest on andesite and basalt flows and make up the south and east wall of the Whitehorse caldera. In the north and west part of the caldera wall, the tuffs rest on older aphyric to porphyritic rhyolite domes and associated flows, unit Ttr_1 on plate 1. To the east and south of the caldera, the tuffs dip toward the caldera and indicate that a zone of subsidence extending several kilometers from the main ring fracture occurs outside the main collapse area. To the southeast of the caldera, the tuff of Whitehorse Creek is considerably thicker and more densely welded as a result of ponding in an oval structural depression.

The ash-flow tuff of Whitehorse Creek is unwelded except for the uppermost part and consists of several individual ash flows and interstratified air-fall tuffs. It has a total minimum thickness of about 65 m. The basal ash flows consist of uncollapsed light-gray pumice and locally abundant lithic fragments in a matrix of fine gray ash. A sequence of air-fall tuffs with a thickness of about 3 m separates the lower ash flows from the upper lithic-rich ash flows. These lithic-rich ash flows are light gray at the base and grade upward into dark-gray to black ash flows. The top of the unit is welded and contains 2 to 3 percent sanidine phenocrysts.

Chemically, the tuff of Whitehorse Creek is similar to the peralkaline base of ash-flow tuff 5 related to the McDermitt caldera complex (table 2). Aluminum is somewhat higher and the contents of trace elements such as Nb indicate that the tuff is as highly differentiated as the McDermitt ash-flow tuff. The thorium content of 21 ppm (parts per million) is similar to the McDermitt tuff and the lower uranium content of 6.9 ppm suggests uranium loss during welding and devitrification.

After collapse of the caldera, ring domes and associated flows and flow breccias were emplaced along the margin of the caldera. These include Flagstaff Butte, Lookout Butte, Red Mountain, Willow Butte, and Whitehorse Butte (pl. 1). The rhyolite domes and associated flows are similar in chemical composition (table 2) and were emplaced at about 14 m.y. as indicated by the 13.8$\pm$.3 m.y. (table 1) age of the dome at Willow Butte. Although the agpaitic coefficient (molecular ratio of Na+K/Al) is less than one, these rhyolites have a peralkaline affinity, and it is likely that sodium has been lost during devitrification. The Nb, Th, and U contents of the domes and flows are comparable to the highest contents found in postcaldera, peralkaline rhyolite intrusives and domes within the McDermitt complex (table 2).

The caldera was subsequently filled with tuffaceous sediments, pyroclastic deposits, diatomites, basalt flows, and palagonite tuffs. The sediments were first described by Smith (1927) and named the Trout Creek Formation. On the basis of a detailed study of the flora within the Trout Creek Formation, MacGinite (1933) assigned a Miocene age to the formation. A basaltic tuff near the top of the formation has been dated at 13.1 m.y. by K-Ar method (Evernden and James, 1964). The base of the formation is in depositional contact with the rhyolite dome and flows of Willow Butte, which have a K-Ar age of 13.8 m.y. Taking into account the analytical uncertainty in the age determinations, the Trout Creek Formation appears to have been deposited in a 0.4 to 1.0 m.y. interval. Only the upper 60 m of the caldera-fill deposits are exposed. In order to test the uranium potential of the caldera-fill deposits the U.S. Department of Energy drilled a 226-m core

Table 2.--Partial chemistry of tuff of Whitehorse Creek, and Willow Butte and Whitehorse Butte ring domes.
[All element contents in percent except for U, Th, and Nb which are in ppm]

	Rhyolite of Willow Butte	Rhyolite of Whitehorse Butte	Tuff of Whitehorse Creek	McDermitt tuff #5	McDermitt rhyolite intrusive
Age	13.8±.3		15.0±.3	15.8±.5	
SiO_2	75.8	76.5	74.8	75.3	75.9
Al_2O_3	12.7	12.3	12.6	11.5	13.3
ΣFe_2O_3	1.83	1.4	2.47	3.25	1.24
MgO	.2	.2	.1	<.1	.1
CaO	.23	.54	.32	.37	.48
Na_2O	3.5	4.3	4.75	4.2	4.3
K_2O	5.57	4.58	4.74	4.97	4.42
MnO	.04	.03	.04	.06	.04
U	9.8	7.3	6.9	9.4	12.1
Th	27.8	20.2	21.00	21.5	30.6
Nb	35.0	31.0	30.0	23.0	36.0
Agpaitic Index		.98	1.02	1.06	

hole, drill hole MC7, in the southwest part of the caldera. The location of the drill hole is shown in plate 1.

LITHOLOGY OF CALDERA-FILL DEPOSITS AND UNDERLYING VOLCANIC ROCKS

Caldera-fill deposits compose the upper 135 m of drill hole MC-7. Because the top of the drill hole is located 10 m above the base of the exposed part of the Trout Creek Formation, the total thickness of the formation is 185 m. The lower 91 m of the core consists of the tuff of Whitehorse Creek and an underlying rhyolite flow (fig. 2). From the base of the hole up to a depth of 183.5 m, the rhyolite flow is gray green to purple, aphyric, and finely flow banded. The top 7.9 m of the flow consists of black perlitic glass that grades downward into maroon lithophysal rhyolite which has undergone vapor phase recrystallization and is commonly fractured. The fractures are coated with montmorillonite and manganese and (or) iron oxide.

Overlying the rhyolite is a 47-m-thick ash-flow tuff sequence (fig. 2). This ash-flow tuff sequence has been correlated with the tuff of Whitehorse Creek on the basis of similar stratigraphy and lithology. The basal 2.2 m consists of poorly sorted unwelded ash-flow tuff in which both the pumice and ash matrix have been altered to salmon-pink clay. Approximately 2 m of drill core above this tuff is missing. From 181.3 to 169.5 m, the core consists of perlitic black obsidian with thin interbeds of pink clay. This interval is overlain by 32.9 m of ash-flow tuff. The lower 8.1 m contains pumice lapilli and abundant lithic fragments with diameters of up to 10 cm. These lithic fragments, which commonly have oxidation rinds, occur in a yellow to light-brown ash matrix. The fragments are considerably smaller (<2 cm) and less abundant in the upper 24.8 m. This upper part contains both light and dark-gray pumice lapilli in an ash matrix that varies in color from dark or light gray to tan or salmon pink. The tuff is partially welded and the lithic fragments are commonly surrounded by black halos.

A sequence of interbedded tuffaceous sedimentary rocks, water-laid tuff, and diatomaceous earth make up the upper part of the drill hole (fig. 2 and pl. 2). These deposits have a total thickness of approximately 135 m. The upper part of this sequence was originally described by MacGinite (1933). The classification scheme used below in describing these tuffaceous sediments and pyroclastic deposits is that of Schmid (1981). Reference may be made to the detailed stratigraphic column of the Whitehorse caldera sediments (pl. 2) for the lithologic description that follows.

The basal 1 m of the caldera-fill sequence consists of tuffaceous breccia composed of volcanic clasts in a yellow-white argillaceous matrix. The breccia grades up section into pumice lapilli-bearing tuffaceous sandstone and siltstone. Overlying these sediments is a 16.3-m-thick sequence (135.6-119.3 m) of interbedded tuffaceous fine-grained sandstone, siltstone, and minor shale. Minor beds of lapilli-ash tuff and clay are also present. Some of the beds contain variable amounts of pumice lapilli as well as fossil plant debris. This interval is characterized by the presence of abundant soft sediment deformation structures; primarily slump structures. The interval between 108.9 and 119.3 m consists of interbedded ash tuff, tuffaceous sandstone and minor shale and clay; one pumice lapilli tuff bed is also present. Graded beds, scour and fill structures, and cross laminations are present. From the top of this interval up to 101.2 m, the drill core is

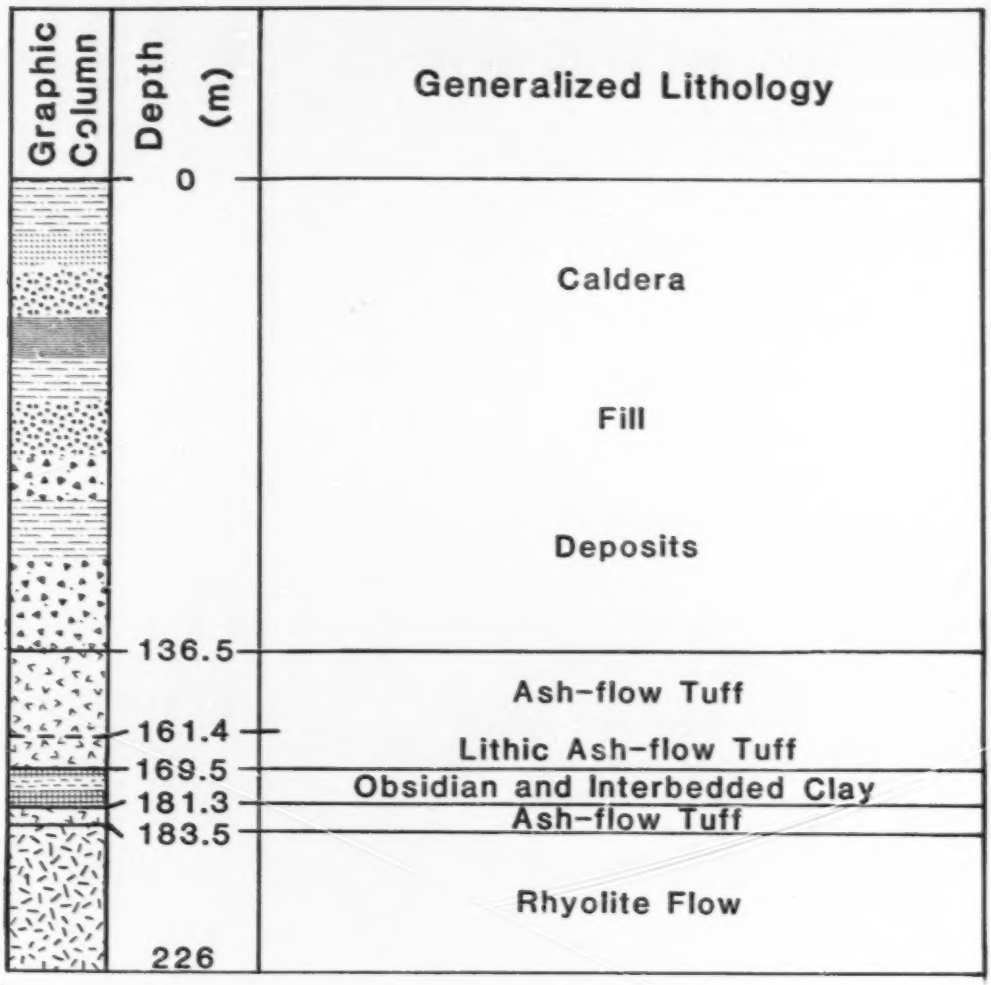

Figure 2.--Generalized lithologic description of drill core.

composed of interbeds of ash, clay, tuffaceous sandstone, siltstone, and minor shale. These beds are generally well laminated. A 14.9-m-thick section of coarse and fine vitric ash comprises the interval from 101.2 to 86.3 m. One 5.9-m-thick graded bed in this interval ranges from pumice lapilli to fine ash. Soft sediment deformation, principally slump structures, is common near the base of the interval. Overlying this section, from 86.3 m to 76.5 m, are ash and pumice lapilli-ash, clay, shale, and siltstone interbeds; many beds are organic rich. This interval contains abundant graded ash beds and minor scour and fill structures and cross laminations. No drill core was recovered between 76.5 and 69.8 m. From the latter depth up to 53.6 m, the core consists of finely laminated ash, tuffaceous sandstone and siltstone, clay, and minor shale interbeds; a few crystal ash beds rich in magnetite and andesine, and biotite and oligoclase are present. The lower 4 m of this section contains abundant fossil plant debris and some graded beds. Above this interval is a 14.1-m-thick section (53.6-39.5 m) of interbedded, partially laminated coarse and fine vitric ash, and minor graded beds of pumice-lapilli ash; some basal clay, siltstone, and diatomaceous earth beds are also present. Minor slump structures and graded beds are found throughout the interval. Overlying this section are interbeds of predominantly graded ash and distomaceous earth; one bed of ash lapilli is also present in this 9-m-thick interval (from 39.5-30.5 m). A 7.2-m-thick layer of coarse vitric ash occurs above this interval in which the lower 80 cm displays graded bedding. Some minor soft sediment deformation structures are also present. From 23.3 m to 1.8 m, the core consists of diatomaceous earth with minor ash and very minor clay, siltstone and shale interbeds. No drill core was recovered between 17.0 m and $\leq$ 11.9 m. The ash beds are commonly graded and a few are diatomaceous. The top 1.8 m of the hole consists of regolith.

INTERPRETATION OF CALDERA-FILL VOLCANIC ROCKS

The lowermost rhyolite flow has been correlated with the older aphyric to porphyritic rhyolites mapped in the wall of the Whitehorse caldera. These flows are part of a rhyolite dome field which formed prior to the development of the Whitehorse caldera and are the oldest rocks exposed in the area of the caldera. Volcanism related to the development of the Whitehorse caldera began with the eruption of a thin ash-flow tuff. Following this initial eruption, thin glassy rhyolite flows and airfall ash were deposited. The first major ash-flow tuff erupted consists of a lower lithic-rich tuff which represents a near-vent facies of the tuff of Whitehorse Creek.

Upon termination of the ash-flow eruption, collapse of the ash-flow tuff and older rocks occured, forming a collapse caldera. A tuffaceous breccia, probably representing caldera wall colluvium, was deposited upon the floor of the caldera. Sediments began to accumulate in a lake in this basin. As a result, finer tuffaceous sediments derived from both the ash-flow tuff and older flows were subsequently deposited in the basin. The water in which these fine-grained sediments were deposited was quiet, although occasionally currents were sufficient to erode small channels on the lake bottom. Ash deposition in the basin resulted from a few minor eruptions. Fossil plant debris suggest that broadleaf plants thrived around the lake. Extreme soft sediment flowage and slumping of these basal sediments occurred and may have been related to earthquakes induced by minor volcanic eruptions and to slope unstability.

Air-fall ash eruptions increased in frequency, resulting in water-laid ash and lapilli ash-tuff deposits. Between eruptions, fine tuffaceous sediments were deposited. Elsewhere in the basin, some minor subaqueous sliding or slumping occurred, resulting in turbidity currents which formed graded beds. The lake water occasionally had enough velocity to form small scour channels and much less frequently cross laminations. Broadleaf plants continued to flourish nearby. Lacustrine sedimentation was abruptly terminated by renewed volcanism and the basin was blanketed with several thick layers of ash; the absence of interbedded epiclastic material indicates that this occurred in a relatively short time span. The sudden increase in quantity of ash deposits at the drill site may have resulted from one or more of the following: (a) occurrence of ash eruptions close to site, (b) increase in volume of ash erupted, or (c) occurrence of ash eruptions from vents on windward side of site. Some of the ash is size graded due to slow settling in the lake. Some of the unsettled ash underwent subaqeous slumping and flowage. After this event, eruptions of ash continued, but only minor amounts were deposited in the basin. Between eruptions, fine-grained tuffaceous sediments were deposited, including organic-rich clay and silt and plant debris. The presence of some crystal-rich ash beds of intermediate to mafic composition within these sediments suggests that minor volcanism of more mafic composition occurred contemporaneously with rhyolitic volcanism. Subaqeous current velocity was great enough at this time to produce cross laminations and small scour channels. This and other temporary increases in current energy may reflect shallowing of the lake along with subaqueous "channeling" of high velocity water originating from nearby stream inlets. Alternately, these strong currents could be a result of density currents near the bottom of the lake. Graded beds within this sequence may have been produced by subaqueous slide-induced turbidity currents. Eventually the lake water became relatively quiet, although some occasional slumping of the sediments occurred.

After a period of quiet lacustrine sedimentation, another thick sequence of ash and minor pumice lapilli-ash was deposited in a relatively short time span, as indicated by the lack of interbedded epiclastic material. Laminations within some of the fine ash as well as the presence of coarse, fine, and graded ash interbeds indicates that both the rate of depositon and the size of the ash particles were somewhat variable. Several of the previously discussed parameters affecting ash deposition could be used to explain these observations. As before, some of this ash was subjected to minor slumping and flowage.

Contemporaneous with the deposition of the thick ash sequence, diatoms appeared in the caldera lake. These organisms accumulated on the floor of the lake and minor ash eruptions disrupted the otherwise continuous deposition of diatoms. Commonly there is a gradual transition from coarse- to fine-ash deposition as a result of the coarser fraction settling out of the ash clouds and through the water before the finer fraction. A final thick graded layer of coarse ash was deposited rapidly in the basin; this deposit was probably the result of a major local ash eruption. Soft sediment slumping and flowage occurred within this layer, possibly as a result of the incoherency and unstability of the ash. Ash eruptions occurred less frequently after this event, and each one resulted in the deposition of only thin ash beds. Between the eruptions, diatoms continued to accumulate within the basin. Very rarely, silt and clay washed into the basin.

ALTERATION MINERALOGY OF CALDERA-FILL DEPOSITS

From the base of the drill hole up to a depth of about 105 m the rocks have been partially altered to clays, potassium feldspar, and (or) zeolites (pl. 2). The mineralogy of the sediments and water-laid pyroclastic deposits forming the upper 136 m of drill core have been studied in detail using both a Rigaku Miniflex X-ray diffraction unit and a scanning electron microscope (SEM). The volcanic flows and deposits below 136 m have been studied only by megascopic means.

The following description and interpretation of the alteration mineralogy of the upper sedimentary section is based on the data presented in plate 2. Each sample collected for X-ray diffraction analysis represents no more than 60 cm of vertical section within the drill core; typically only 2 cm of core have been sampled. The average vertical separation between samples is about 1.25 m in the lower altered part of the sedimentary section and about 7 m in the upper unaltered part. Samples were taken where major changes in mineralogy and (or) lithology occur. Samples representing more than 2 cm of core are composite samples of the various rock types within the sample interval. Because of this sampling procedure, it is possible that some trends or patterns in alteration mineralogy could be overlooked or appear to be insignificant. In the mineralogy plots in plate 2, adjacent X-ray peak heights for each mineral or the glass have been connected with light weight lines to indicate the uncertainty in the alteration trends between analyzed samples.

As indicated by the plot of glass and amorphous silica, the sediment and pyroclastic deposits that make up the upper 110 m of core are composed primarily of unaltered glass shards or amorphous silica, as diatomaceous earth. Clay peaks in this upper section correspond to layers of claystone, siltstone, or shale. Megascopically, the ash appears fresh and is very friable. The only indication of devitrification of glass shards occurs at a depth of about 110 m, where some of the glass has been altered to cristobalite. Minor cristobaltie was also identified only on the SEM at a depth of 125 m.

Below 108 m the deposits have generally been altered. Most of the sediments and water-laid tuffs below this depth contain varying amounts of clay, which is almost exclusively montmorillonite. The highest concentrations of montmorillonite are typically found in clay, siltstone, or shale beds. Although some of the clay is dioctahedral, most of it is mixed layer or trioctahedral. From the plot of depth versus montmorillonite structure, a cyclic pattern emerges; the clays change with depth from dioctahedral through mixed-layer to trioctahedral and then back to dioctahedral. There appears to be no correlation between these "cycles" and changes in zeolite assemblages or lithology. Kaolinite was detected in two samples.

In a layer of black clay just below 108 m, pyrite aggregates were identifed on the SEM. Pyrite was also detected in a black clay layer at a depth of about 131 m. These and other black clay layers in between are interbedded with organic-rich sediments. Some of this organic material was probably replaced by pyrite as a result of bacterial decomposition in a reducing environment.

Zeolitic alteration begins at 111 m, about 3 m below the depth where clay alteration begins. Both phillipsite and erionite are present. At a depth of 113 m, clinoptilolite occurs along with these two zeolites. Both erionite and clinoptilolite are locally present throughout the remainder of the altered lacustrine deposits, but phillipsite abruptly terminates at a depth of about 118 m. Although neither of the former zeolites are ubiquitous within the altered zone, clinoptilolite is somewhat more common. Adularia is present in most of the lower lake deposits, beginning at a depth of about 120 m. Adularia and erionite almost always occur together and their relative concentrations appear to correlate with one another with changes in depth. The interval between 127.6 or 130.8 m consists primarily of shale and siltstone composed of dioctahedral montmorillonite and lacks any zeolites. To summarize, these alteration mineral assemblages consist of three types: (1) montmorillonite, (2) phillipsite$\pm$montmorillonite$\pm$clinoptilolite$\pm$erionite, and (3) clinoptilolite$\pm$montmorillonite$\pm$erionite$\pm$adularia.

Scanning Electron Microscopy observations

Crystal forms and habits as well as textural relationships of most of the minerals detected by X-ray diffraction were observed by Scanning Electron Microscopy (SEM). Erionite typically occurs as a partial replacement of glass shards; bundles of erionite can usually be identified within the shards (fig. 3). It is also observed as needlelike crystals occurring together in bundles along with montmorillonite in cavities within the rock (fig. 4). Uncommonly, this zeolite occurs as individual needles that are attached lengthwise to the crystal faces of clinoptilolite prisms exposed in cavities.

Unlike erionite or clinoptilolite, individual crystals of phillipsite are rarely observed at even high magnification under the SEM. However, rather large concentrations of phillipsite have been detected in these samples by X-ray diffraction analysis and suggests that phillipsite occurs as extremely minute crystals that either pseudomorphically replace the glass shards or are disseminated throughout the surrounding clay. Phillipsite that has been observed occurs as bundles of somewhat planar to tabular crystals (fig. 5).

Clinoptilolite commonly occurs as euhedral crystals having tabular to prismatic crystal habit. This zeolite commonly occurs as aggregates of interlocking crystals within cavities (fig. 6) or as individual crystals coated with clay. Like phillipsite, large concentrations of clinoptilolite have been detected by X-ray diffraction analysis in most SEM samples. No clinoptilolite, however, was observed under the SEM in some of these samples. Possibly this zeolite occurs as pseudomorphs after glass or as finely disseminated minute crystals.

Most of the SEM samples contain abundant clay that typically occurs in aggregates displaying boxwork morphology (fig. 7). Distinguishing detrital clay from secondary clay on the SEM is not usually possible. Most commonly the zeolites and potassium feldspar are intergrown with clay minerals.

Adularia occurs in the form of very minute rhombohedrons which are intergrown with clay mineral aggregates (fig. 8). This phase is rarely observed bacause the crystals are too small to be resolved on the SEM.

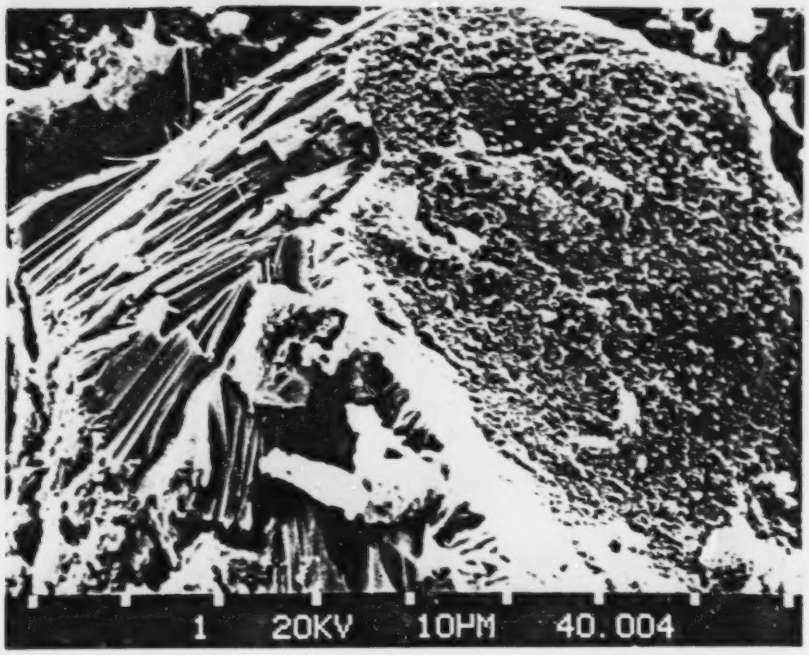

Figure 3.--SEM photo of erionite replacing a glass shard. Distance between the marks is 10 μm.

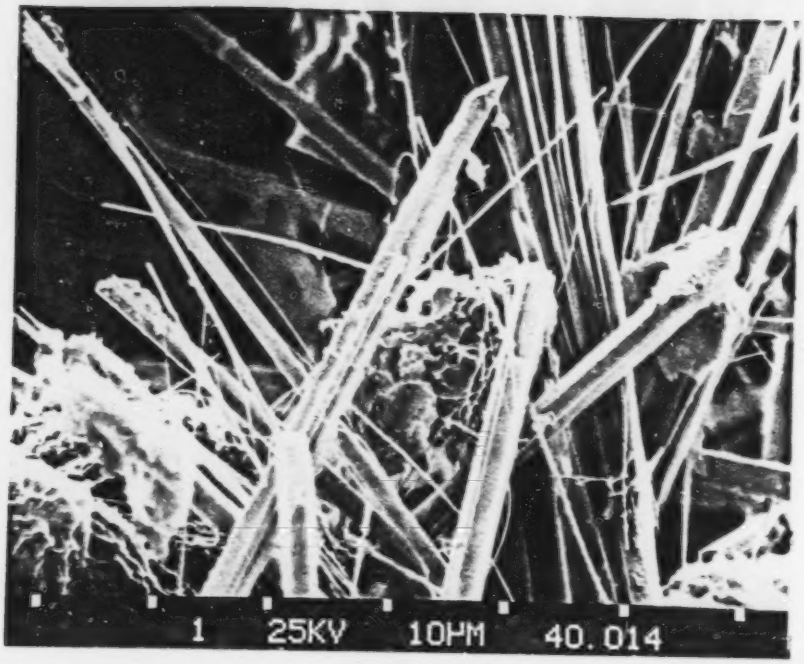

Figure 4.--SEM photo of erionite and montmorillonite filling cavities in the rock. Distance between tic marks is 10 μm.

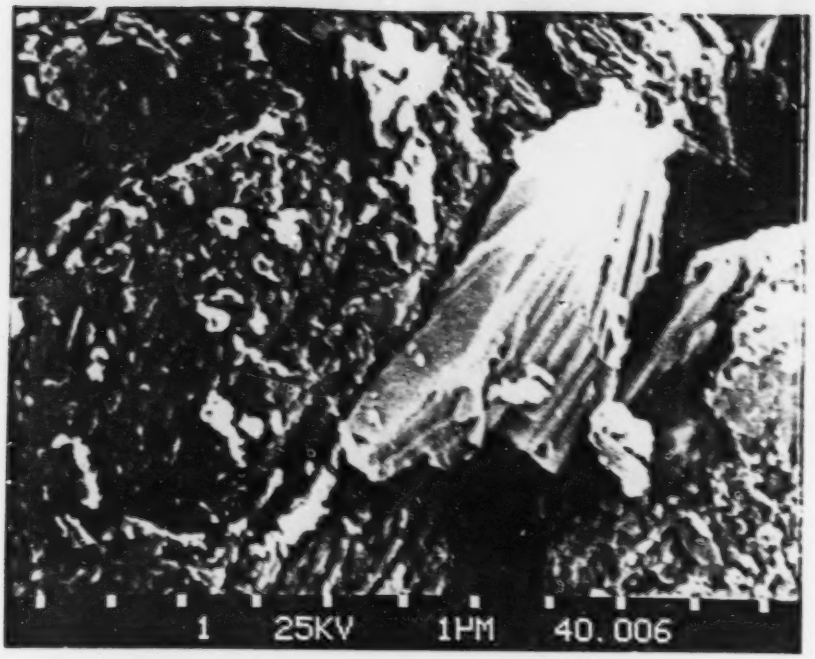

Figure 5.--SEM photo of phillipsite crystals. Distance between tic marks is 1 μm.

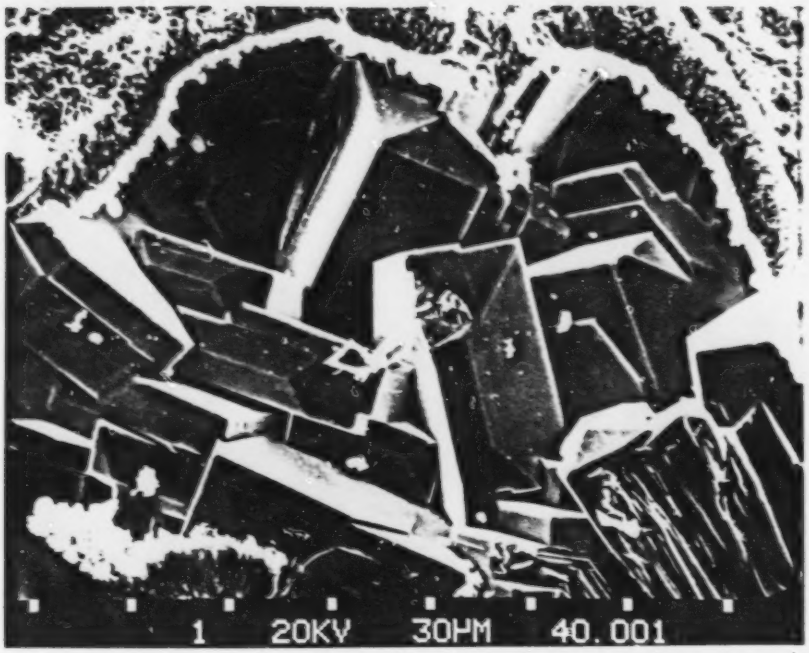

Figure 6.--SEM photo of clinoptilolite crystals filling cavities. Distance between tic marks is 30 μm.

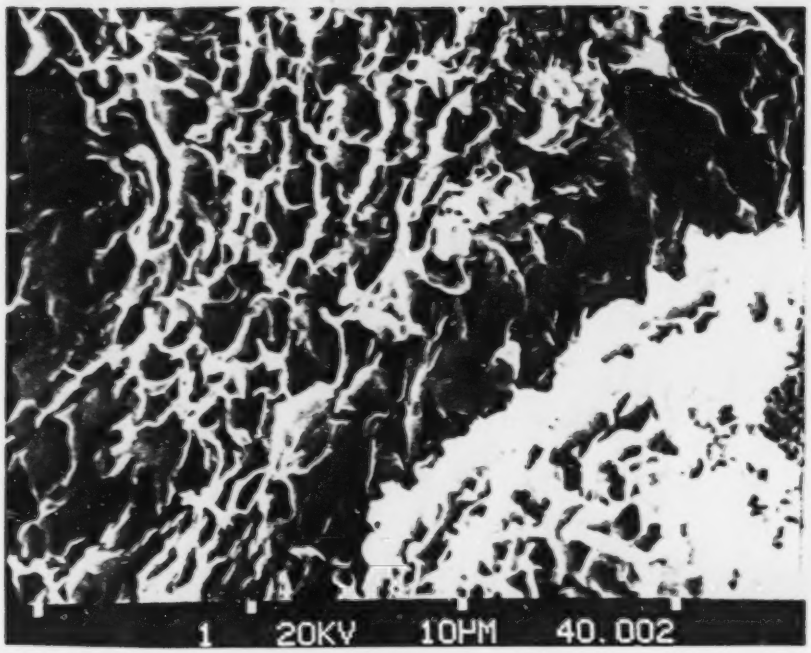

Figure 7.--SEM photo of montmorillonite clay. Distance between tic marks is 1 µm.

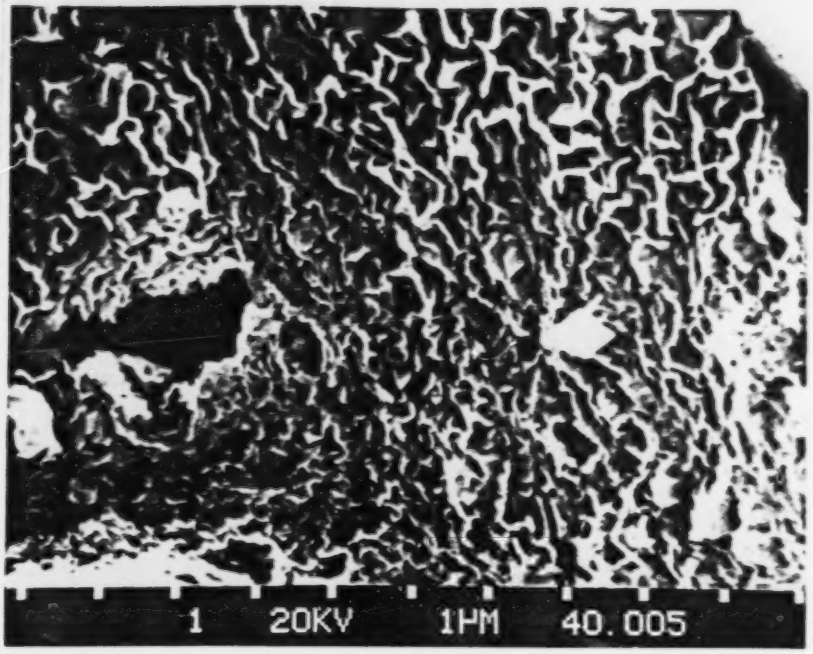

Figure 8.--SEM photo of adularia amd typical clay mineral morphology. Distance between tic marks is 1 µm.

Within the drill core the tuff of Whitehorse Creek has undergone argillic alteration; most of the ash and pumice lapilli have been altered to clay. The glass layers are partly hydrated and display perlitic texture. In light of the vertical distribution of zeolites in the overlying lacustrine deposits, these lower volcanic rocks have probably undergone zeolitic alteration as well.

A vertical mineral zonation within the core is defined by the change from unaltered caldera-fill deposits in the upper part to altered deposits showing a regular distribution of the alteration minerals in the lower part. On the basis of this evidence alone, it is not clear if these deposits were altered diagenetically, hydrothermally, or both.

Uranium potential of caldera-fill deposits

Pyroclastic deposits and rhyolite domes within the Whitehorse caldera have high uranium and thorium contents. Chemically these volcanic rocks are similar to those associated with the McDermitt caldera complex which hosts several uranium occurrences and deposits. In the Whitehorse caldera, extensive silicification of caldera-fill deposits adjacent to Flagstaff Butte has resulted in the formation of several large opalite masses. The silicification, and possibly the zeolitization, indicate that a large hydrothermal system was once active along the southwest margin of the caldera. Although uranium in the volcanic rocks was likely mobilized during hydrothermal alteration and zeolitization, no anomalous zones were encountered in radiometric logging of the drill hole. The presence of several organic and pyritic zones within the caldera-fill deposits indicate that beds favorable for concentrating uranium are present within the basin. Because the caldera has been only partly disrupted by recent faulting, it has remained essentially a closed basin to the present and may still contain a uranium resource elsewhere in the basin.

ACKNOWLEDGMENTS

Our gratitude is extended to the U.S. Department of Energy for providing the drill core, and to personnel with Bendix Field Engineering for their cooperation in this study. Funding for this project was provided by the U.S. Department of Energy.

REFERENCES

Evernden, J. F., and James, G. T., 1964, Potassium-argon dates and the Tertiary floras of North America: American Journal of Science, v. 262, p. 945-974.

MacGinite, H. D., 1933, The Trout Creek flora of southeastern Oregon: Carnegie Institution of Washington Publication 416, no. 2, p. 21-68.

MacLeod, N. S., Sherrod, D. R., Chitwood, L. A., and McKee, E. H., 1981, Roadlog for Newberry volcano, Oregon, in Guides to some volcanic terranes in Washington, Idaho, Oregon, and northern California: U.S. Geological Survey Circular 838, p. 85-103.

Rytuba, J. J., and Glanzman, R. K., 1979, Relation of mercury, uranium, and lithium deposits to the McDermitt caldera complex, Nevada-Oregon: Nevada Bureau of Mines and Geology Report 33, p. 109-118.

Schmid, R., 1981, Descriptive nomenclature and classification of pyroclastic deposits and fragments: Recommendations of the IUGS Subcommission on the systematics of igneous rocks: Geology, v. 9, p. 41-43.

Smith, W. D., 1927, Contributions to the geology of southeastern Oregon: Journal of Geology, v. 35, p. 421-441.

Walker, G. W., 1974, Some implications of late Cenozoic volcanism to geothermal potential in the high lava plains of south-central Oregon: Ore Bin, v. 36, p. 109-119.

Walker, G. W. and Nolf, B., 1981, Roadlog for High Lava Plains, Brothers fault zone to Harney Basin, Oregon, in Guides to some volcanic terranes in Washington, Idaho, Oregon, and northern California: U.S. Geological Survey Circular 838, p. 105-111.

DEPARTMENT OF THE INTERIOR
UNITED STATES GEOLOGICAL SURVEY

PLATE 1 OF 2
OPEN-FILE REPORT 81-1092

DESCRIPTION OF MAP UNITS

Qal Alluvium
Qt Alluvium and talus
QTg Unconsolidated conglomerate
Tb2 Basalt flow
Tsa Trout Creek Formation,silicified
Ttc Trout Creek Formation
Ttrw Rhyolite domes and flows
Tt6 Ash-flow tuff of Whitehorse Creek
Taf Andesite flow
Tb1 Basalt flows
Tt5 Ash-flow tuff 5
Tt4 Ash-flow tuff 4
Ttu Ash-flow tuff undifferentiated
Ta Andesite and basaltic andesite flows
Tpa Porphyritic andesite flow
Ttr1 Rhyolite domes and flows

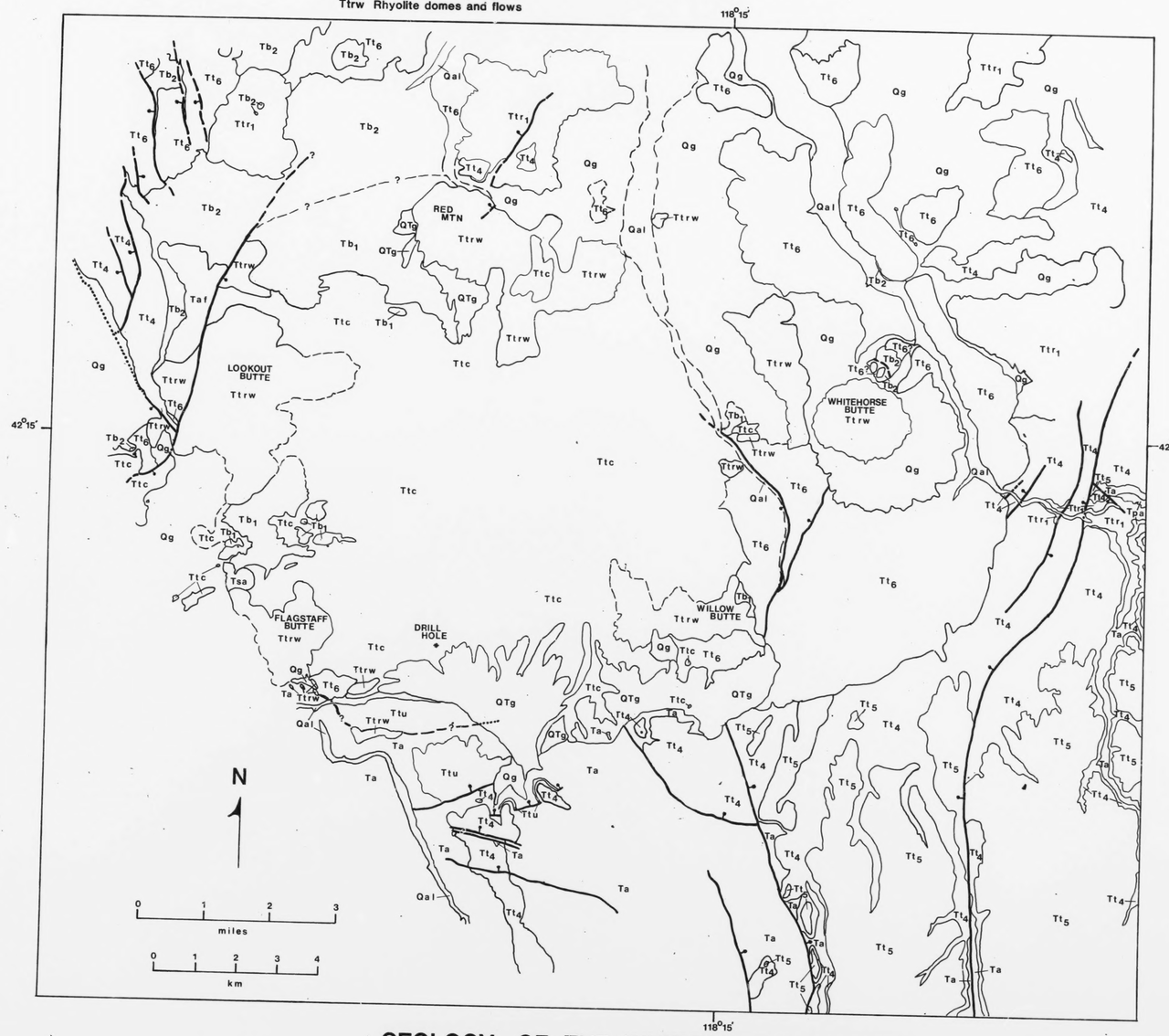

GEOLOGY OF THE WHITEHORSE CALDERA

DEPARTMENT OF THE INTERIOR
UNITED STATES GEOLOGICAL SURVEY

OPEN-FILE REPORT
81-1092

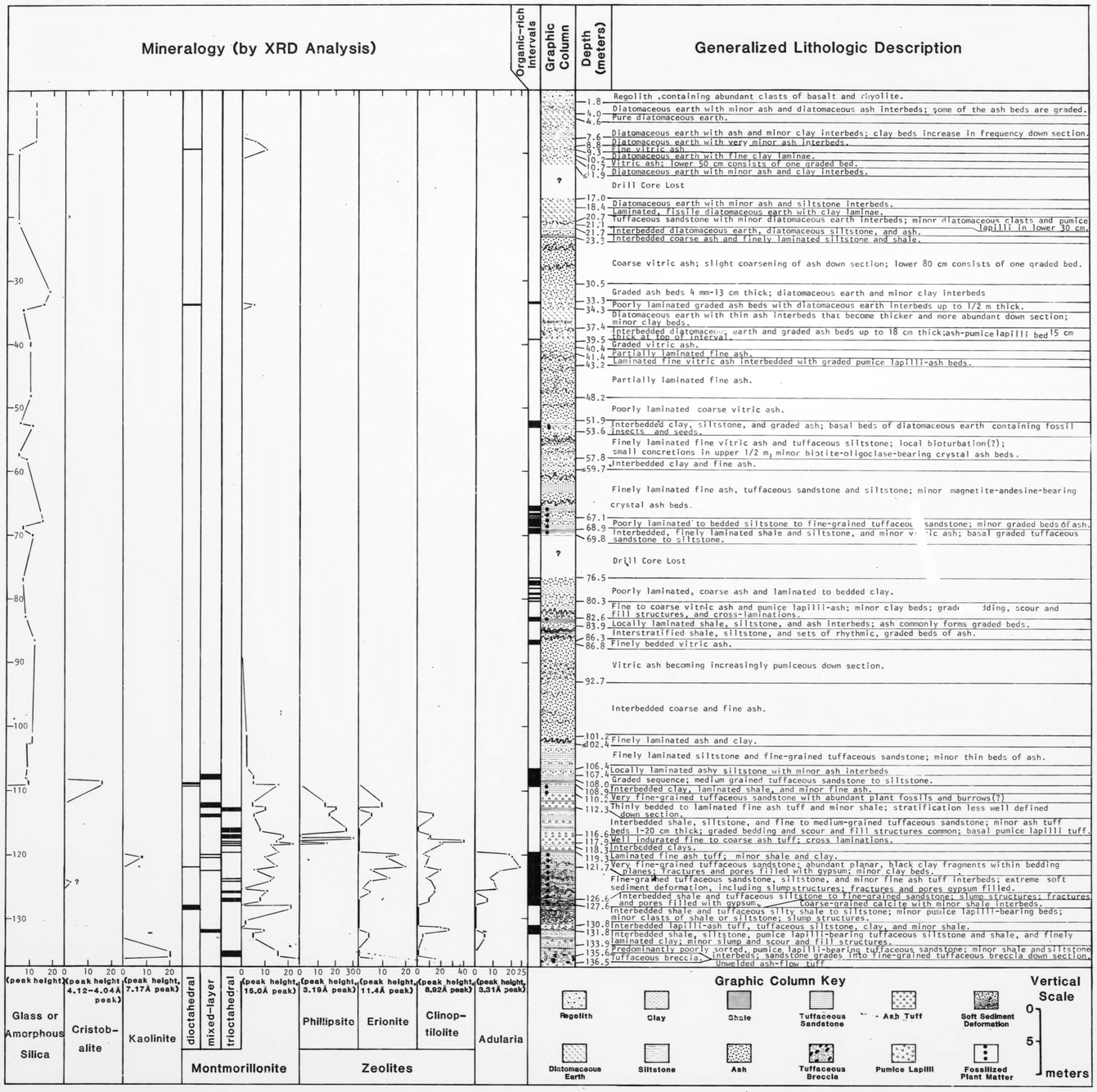
Mineralogy (by XRD Analysis)
Organic-rich Intervals
Graphic Column
Depth (meters)
Generalized Lithologic Description
Regolith ,containing abundant clasts of basalt and rhyolite.
1.8
Diatomaceous earth with minor ash and diatomaceous ash interbeds; some of the ash beds are graded.
4.0
Pure diatomaceous earth.
4.6
Diatomaceous earth with ash and minor clay interbeds; clay beds increase in frequency down section.
7.6
Diatomaceous earth with very minor ash interbeds.
8.8
Fine vitric ash.
9.3
Diatomaceous earth with fine clay laminae.
10.2
Vitric ash; lower 50 cm consists of one graded bed.
10.7
≤11.9
Diatomaceous earth with minor ash and clay interbeds.
Drill Core Lost
17.0
Diatomaceous earth with minor ash and siltstone interbeds.
18.4
Laminated, fissile diatomaceous earth with clay laminae.
20.7
Tuffaceous sandstone with minor diatomaceous earth interbeds; minor diatomaceous clasts and pumice lapilli in lower 30 cm.
21.1
Interbedded diatomaceous earth, diatomaceous siltstone, and ash.
21.7
Interbedded coarse ash and finely laminated siltstone and shale.
23.5
Coarse vitric ash; slight coarsening of ash down section; lower 80 cm consists of one graded bed.
30.5
Graded ash beds 4 mm-13 cm thick; diatomaceous earth and minor clay interbeds
33.3
Poorly laminated graded ash beds with diatomaceous earth interbeds up to 1/2 m thick.
34.3
Diatomaceous earth with thin ash interbeds that become thicker and more abundant down section; minor clay beds.
37.4
Interbedded diatomaceous earth and graded ash beds up to 18 cm thick;ash-pumice lapilli bed 15 cm thick at top of interval.
39.5
Graded vitric ash.
40.4
Partially laminated fine ash.
41.4
Laminated fine vitric ash interbedded with graded pumice lapilli-ash beds.
43.2
Partially laminated fine ash.
48.2
Poorly laminated coarse vitric ash.
51.9
Interbedded clay, siltstone, and graded ash; basal beds of diatomaceous earth containing fossil insects and seeds.
53.6
Finely laminated fine vitric ash and tuffaceous siltstone; local bioturbation(?); small concretions in upper 1/2 m, minor biotite-oligoclase-bearing crystal ash beds.
57.8
≤59.7
Interbedded clay and fine ash.
Finely laminated fine ash, tuffaceous sandstone and siltstone; minor magnetite-andesine-bearing crystal ash beds.
67.1
Poorly laminated to bedded siltstone to fine-grained tuffaceous sandstone; minor graded beds of ash.
68.9
Interbedded, finely laminated shale and siltstone, and minor vitric ash; basal graded tuffaceous
69.8
sandstone to siltstone.
Drill Core Lost
76.5
Poorly laminated, coarse ash and laminated to bedded clay.
80.3
Fine to coarse vitric ash and pumice lapilli-ash; minor clay beds; grade bedding, scour and fill structures, and cross-laminations.
82.6
83.9
Locally laminated shale, siltstone, and ash interbeds; ash commonly forms graded beds.
86.3
Interstratified shale, siltstone, and sets of rhythmic, graded beds of ash.
86.8
Finely bedded vitric ash.
Vitric ash becoming increasingly pumiceous down section.
92.7
Interbedded coarse and fine ash.
101.2
≤102.4
Finely laminated ash and clay.
Finely laminated siltstone and fine-grained tuffaceous sandstone; minor thin beds of ash.
106.4
Locally laminated ashy siltstone with minor ash interbeds
107.4
Graded sequence; medium grained tuffaceous sandstone to siltstone.
108.0
Interbedded clay, laminated shale, and minor fine ash.
108.9
Very fine-grained tuffaceous sandstone with abundant plant fossils and burrows(?)
110.2
Thinly bedded to laminated fine ash tuff and minor shale; stratification less well defined down section.
112.3
Interbedded shale, siltstone, and fine to medium-grained tuffaceous sandstone; minor ash tuff beds 1-20 cm thick; graded bedding and scour and fill structures common; basal pumice lapilli tuff.
116.6
Well indurated fine to coarse ash tuff; cross laminations.
117.9
Interbedded clays.
118.3
Laminated fine ash tuff; minor shale and clay.
119.5
Very fine-grained tuffaceous sandstone; abundant planar, black clay fragments within bedding planes; fractures and pores filled with gypsum; minor clay beds.
121.7
Fine-grained tuffaceous sandstone, siltstone, and minor fine ash tuff interbeds; extreme soft sediment deformation, including slump structures; fractures and pores gypsum filled.
126.6
Interbedded shale and tuffaceous siltstone to fine-grained sandstone; slump structures; fractures and pores filled with gypsum.
127.6
Coarse-grained calcite with minor shale interbeds.
Interbedded shale and tuffaceous silty shale to siltstone; minor pumice lapilli-bearing beds; minor clasts of shale or siltstone; slump structures.
130.8
Interbedded lapilli-ash tuff, tuffaceous siltstone, clay, and minor shale.
131.8
Interbedded shale, siltstone, pumice lapilli-bearing tuffaceous siltstone and shale, and finely laminated clay; minor slump and scour and fill structures.
133.9
Predominantly poorly sorted, pumice lapilli-bearing tuffaceous sandstone; minor shale and siltstone
135.6
Tuffaceous breccia
Interbeds; sandstone grades into fine-grained tuffaceous breccia down section.
136.5
Unwelded ash-flow tuff
30
40
50
60
70
80
90
100
110
120
130
10 20 0 (peak height)
Glass or Amorphous Silica
10 20 0 (peak height, 4.12-4.04Å peak)
Cristobalite
10 20 0 (peak height, 7.17Å peak)
Kaolinite
dioctahedral
mixed-layer
trioctahedral
0 10 20 0 (peak height, 15.0Å peak)
Montmorillonite
10 20 30 0 (peak height, 3.19Å peak)
Phillipsite
10 20 0 (peak height, 11.4Å peak)
Erionite
20 40 0 (peak height, 8.92Å peak)
Clinoptilolite
Zeolites
10 20 25 0 (peak height, 3.31Å peak)
Adularia
Graphic Column Key
Regolith
Clay
Shale
Tuffaceous Sandstone
Ash Tuff
Soft Sediment Deformation
Diatomaceous Earth
Siltstone
Ash
Tuffaceous Breccia
Pumice Lapilli
Fossilized Plant Matter
Vertical Scale
0
5
meters

GEOLOGY AND MINERALOGY OF WHITE HORSE CALDERA SEDIMENTS